A Study of Integration of Parasitic Cancellation Techniques for EMI Filter Design With Discrete Components

Shuo Wang, *Senior Member, IEEE*, Fred C. Lee, *Fellow, IEEE*, and Jacobus Daniel van Wyk, *Fellow, IEEE*

***Abstract*—In this paper, effects of parasitic parameters on the electromagnetic interference (EMI) filter performance are first discussed. The parasitic cancellation techniques for both self- and mutual parasitics are then reviewed and their constraints are identified. The possibilities of integrating parasitic cancellation techniques into one EMI filter are analyzed. It is found that three parasitic cancellation techniques can be integrated into one EMI filter to improve both differential-mode and common-mode filter performances without any conflicts and compromises. Experiments are finally carried out to verify the integration of these three cancellation techniques.**

***Index Terms*—Electromagnetic interference (EMI) filter, equivalent parallel capacitance (EPC), equivalent series inductance (ESL), mutual coupling, parasitic cancellation.**

I. Introduction

ELECTROMAGNETIC interference (EMI) filters are widely used in power electronics systems for EMI noise suppression. Conventional passive EMI filters are one- or two-stage *LC* filters. EMI filters are usually composed of common-mode (CM) and differential-mode (DM) filters. CM filters are used to suppress CM noise, which propagates through the parasitic capacitance between the power electronics systems, ground, line impedance stabilization networks (LISNs), and the power lines. The capacitance of the CM filter is usually limited by the safety standard, such as IEC60950-1. As a result, the total CM capacitance cannot be too large. In order to get a low corner frequency to achieve high attenuation of the CM noise, the CM inductance in CM filters is usually relatively large (for example, 3 mH). DM filters are used to suppress DM noise, which propagates between two power lines. For DM filters, the capacitance of the DM capacitors does not have very strict limitations. It is loosely limited by power factor, inrush current, size, etc. As a result, the total DM capacitance can be more than 1 μF in many applications. To achieve the attenuation needed to meet EMI standards, the DM inductance in DM filters may therefore not need to be very large (for example, 20 μH is enough). Because of this, the DM inductor can be integrated with the CM inductor. Since the two CM inductor windings are directly coupled on a ferrite core, the leakage between these windings is used as a DM inductor.

The inductors and capacitors in EMI filters are not ideal components. First, they have self-parasitics. For capacitors, the equivalent series inductance (ESL) is very important for their performance. For inductors, the equivalent parallel capacitance (EPC) is very important for their performance. Second, there are parasitic couplings between individual components. Two mutual couplings: 1) the mutual inductance between DM inductors and DM capacitors and 2) the mutual inductance between two DM capacitors, are the most important for DM filters [1]. The coupling between the input and output loops of the filters are also important [1], and they can be minimized by minimizing the input and output loop areas. For DM EMI filters, if the DM inductance is the leakage of the CM inductor and the physical dimensions of the DM capacitors are appreciable, the mutual couplings would be significant, due to stray magnetic flux pickup by the DM capacitors. For CM filters, the EPC of the CM inductors is usually the most important parasitic parameter since it may resonate with the CM inductance at very low frequencies [2] that degrade the filter's HF performance. The magnetic flux of the CM current is contained inside the magnetic cores of the CM inductors, and consequently, does not easily couple to other components.

Fig. 1 shows a typical one-stage single-phase power-line filter that has the same structure as that analyzed earlier. DM inductors are the leakage of the CM inductors. ESL_1, ESL_2, and EPC are the self-parasitics of the components. It should be pointed out that the EPC of the DM inductors is different from that of CM inductors [5], although there is only an EPC shown in Fig. 1. Fig. 2 shows the insertion gains of the DM filter part. Three curves are shown in Fig. 2. The first one is the ideal insertion gain of the filter, the second one is the simulated insertion gain with self-parasitics only, and the third one is a measured insertion gain, which includes both self- and mutual parasitic couplings. Fig. 3 shows the insertion gains of the CM filter part. Three curves are shown in Fig. 3. The first one is the ideal insertion gain, the second one is the simulated insertion gain with self-parasitics, and the third one is the measured insertion gain.

Fig. 2 experimentally shows that the mutual couplings between components determine the DM filter's HF performance. Effects of ESL and EPC on filter performance are not significant unless the mutual couplings are reduced greatly. On the

Manuscript received December 22, 2007; revised April 21, 2008. First published November 17, 2008; current version published December 9, 2008. Recommended for publication by Associate Editor B. Ferreira.

S. Wang and F. C. Lee are with the Center for Power Electronics Systems, Virginia Polytechnic Institute and State University, Blacksburg, VA 0179 USA (e-mail: shuowang@ieee.org).

J. D. van Wyk is with the Center for Power Electronics Systems, Virginia Polytechnic Institute and State University, Blacksburg, VA 0179 USA, and also with the Department of Electrical and Electronic Engineering Science, University of Johannesburg, Johannesburg 524, South Africa.

Color versions of one or more of the figures in this paper are available online at http://ieeexplore.ieee.org.

Digital Object Identifier 10.1109/TPEL.2008.2005382

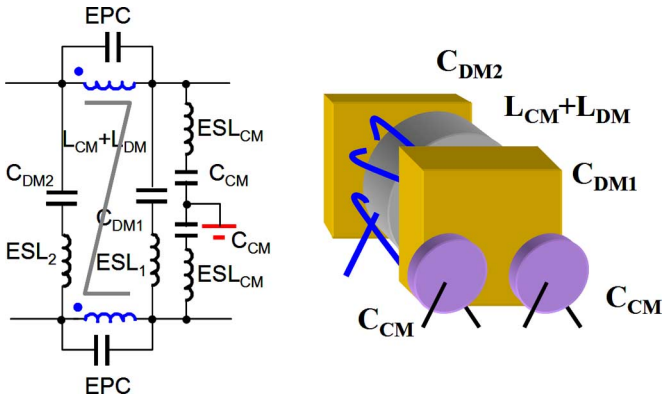

Fig. 1. Typical one-stage single-phase power-line filter in power electronics systems.

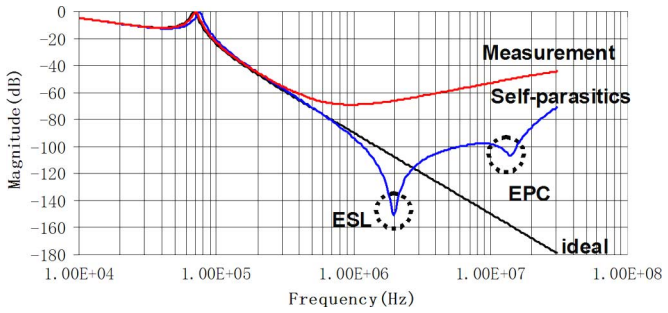

Fig. 2. Effects of parasitics on the DM filter insertion gains.

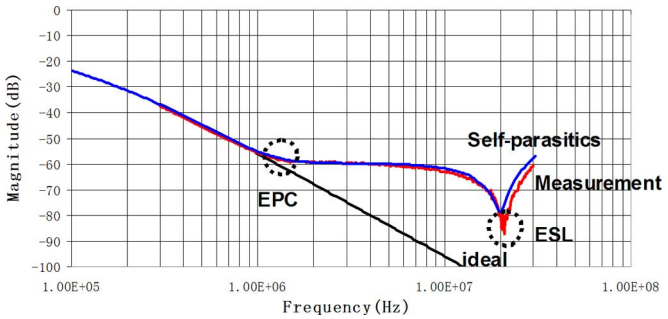

Fig. 3. Effects of parasitics on the CM filter insertion gains.

contrary, for the CM filter in Fig. 3, the measured insertion gain can well match the simulated insertion gain with self-parasitics only. This indicates that the mutual couplings in CM filters are not as important as those in DM filters for the filter under investigation.

In order to improve the DM filter performance, mutual parasitic couplings between components should be reduced first. Only after the mutual couplings are reduced can ESL and EPC reduction have significant improvement on filter performance. On the other hand, in order to improve the CM filter performance, self-parasitics, especially the EPC of inductors, should be reduced.

Many techniques have been developed to cancel mutual parasitic couplings and self-parasitics in EMI filters [3]–[8]. These techniques have been theoretically proved and experimentally verified. However, how to efficiently apply them into EMI filter

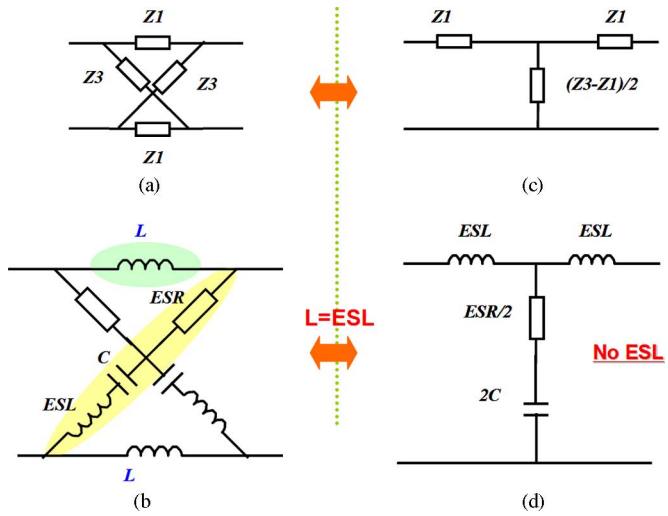

Fig. 4. ESL cancellation for capacitors.

design has not been investigated. There are some issues that need to be addressed. For example, can these techniques be used together without any conflicts? Can these techniques be applied to both DM and CM filters at the same time? This paper will first review the developed parasitic cancellation techniques. The possibilities to integrate them are then investigated. Some conclusions are drawn based on the analysis. Experiments are finally carried out to verify the analysis.

II. Review of Parasitic Cancellation Techniques

In this section, self-parasitic cancellations and mutual parasitic cancellations will be reviewed, and the constraints for their applications will be addressed.

A. ESL Cancellation for Capacitors

ESL cancellation techniques have been reported in [3] and [4]. Basically, the effects of ESL can be canceled using either an X–capacitor–inductor structure [3] or mutual inductance [4]. This paper will review the method of using X–capacitor–inductor structure only. Fig. 4 shows the ESL cancellation concept.

In Fig. 4(a) and (b), two capacitors are connected diagonally. ESR is the equivalent series resistance of the capacitors. Two small inductors L, which can be made using printed circuit board (PCB) traces, are connected to the top and bottom sides. If the inductance of these two inductors is equal to ESL, the resultant circuit is a π-type filter without the effects of ESL, as shown in Fig. 4(c) and (d). In experiments, it has been proven that the ESL cancellation is effective for the suppression of HF noise when the effects of the mutual couplings between the capacitors and other components are negligible. Its typical applications include the noise suppression capacitors in bus bars, input bulk capacitors of converters, and the input capacitors of boost power factor correction (PFC) converters. For these applications, the mutual couplings between the ESL-canceled capacitors and other components are small.

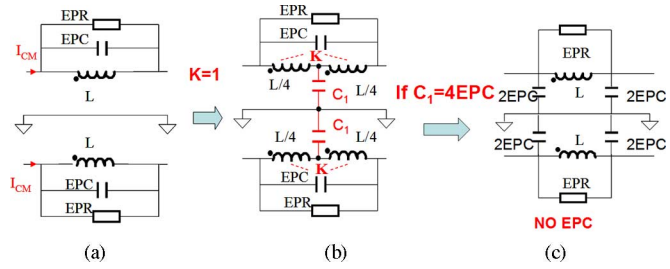

Fig. 5. EPC cancellation for CM inductors.

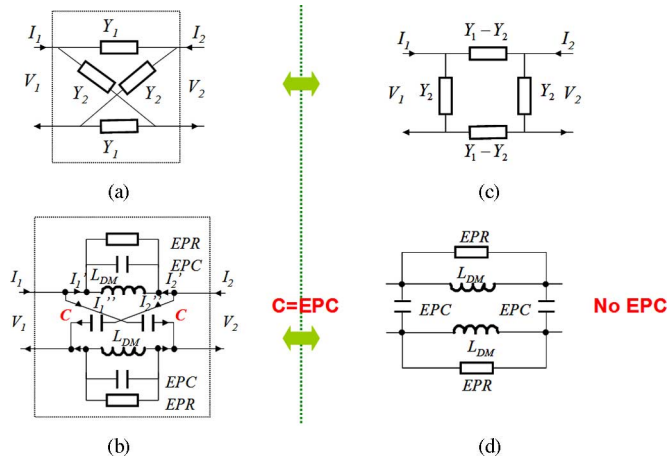

Fig. 6. EPC cancellation for DM inductors.

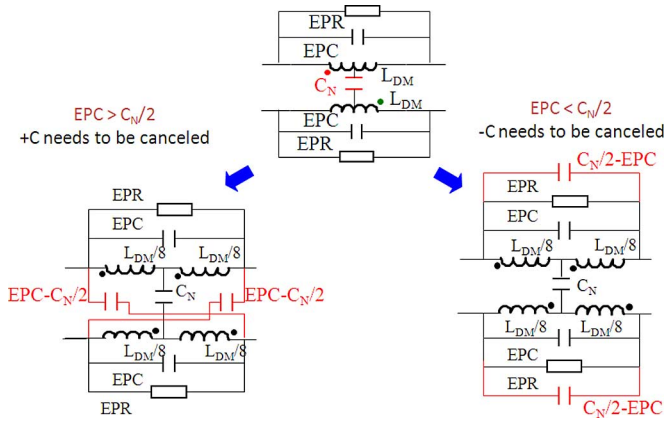

Fig. 7. EPC cancellation for coupled DM inductors.

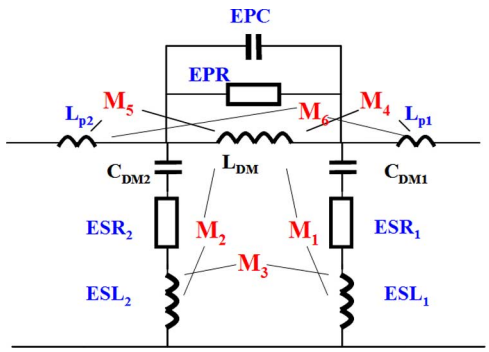

Fig. 8. Parasitic model of the DM filter.

B. EPC Cancellation for Inductors

EPC cancellation techniques have been reported in [5]–[7]. This paper will review the methods developed in [5] and [7]. The effects of EPC of a CM inductor can be canceled with a grounded capacitor, whose capacitance is four times the value of EPC, connected to the center tap of the CM inductor winding. The winding is made with a bifilar structure to maximize the coupling coefficient between the two winding halves. The concept is shown in Fig. 5. In Fig. 5, EPR represents the equivalent parallel resistance of the inductors. The same cancellation technique can also be applied to DM inductors in some applications [10]. For separate DM filters, each line usually has an identical DM inductor for balance purposes, since an unbalanced filter structure will cause mode transformations between DM and CM noise, which makes the noise suppression difficult [9]. If these two DM inductors are two separate (noncoupled) inductors, the X–capacitor structure can be applied for EPC cancellation. The concept is shown in Fig. 6. In Fig. 6, two cancellation capacitors C, whose capacitance is equal to the EPC, are diagonally connected to two DM inductors. The resultant circuit is a π-type filter without the effects of EPC.

If two DM inductors are coupled, the cancellation is more complicated. In Fig. 7, there is parasitic capacitance C_N between two coupled windings. This capacitance represents the total effects of the direct capacitance between the two windings and the capacitance via the magnetic core. If C_N is less than twice the value of EPC, the method in Fig. 6 still applies. Two capacitors with capacitance equal to the difference between the EPC and half of C_N are diagonally connected to the DM inductors for cancellation. However, if C_N is larger than twice the value of EPC, a capacitor with capacitance equal to the difference between the EPC and half of C_N is paralleled to the inductor on each side to cancel the effects of parasitic capacitance [5].

The EPC cancellation techniques have been proven effective for HF noise suppression when the mutual couplings between the inductors and other components are negligible [5]. A typical application is the EPC cancellation for CM inductors in EMI filters. In this application, the mutual couplings between the EPC-canceled CM inductors and other CM components are small, because the CM magnetic flux is contained within the core.

C. Cancellation of the Mutual Inductance Between Inductors and Capacitors

The parasitic model for the DM filter part in Fig. 1 is shown in Fig. 8, with the mutual parasitic magnetic coupling indicated. In Fig. 8, M_1 and M_2 are the mutual inductance between DM inductor $L_{\rm DM}$ and DM capacitors $C_{\rm DM1}$ and $C_{\rm DM2}$, respectively. Effects of M_1 and M_2 are significant because of two reasons. First, physical dimensions of DM capacitors are large, so DM capacitors easily couple stray magnetic flux. Second, the DM magnetic flux, which is the leakage of the CM inductor, is extended into air, so it easily couples DM capacitors. Depending on the directions of the windings, M_1 and M_2 could be positive or negative. Their effects are equivalent to an inductance, which is equal to M_1 or M_2, in series with the DM capacitors. Since

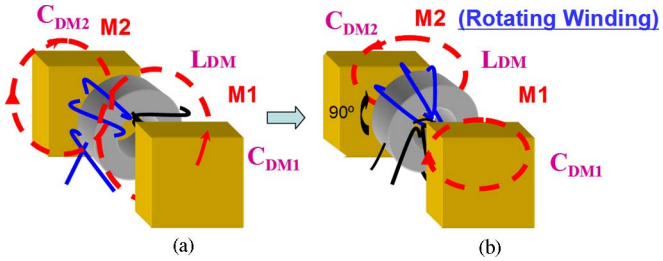

Fig. 9. Minimization of M_1 and M_2 by rotating winding by 90°.

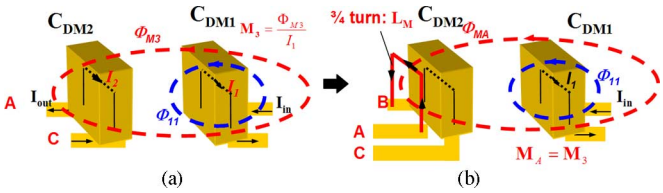

Fig. 10. Canceling effects of M_3 with cancellation turn.

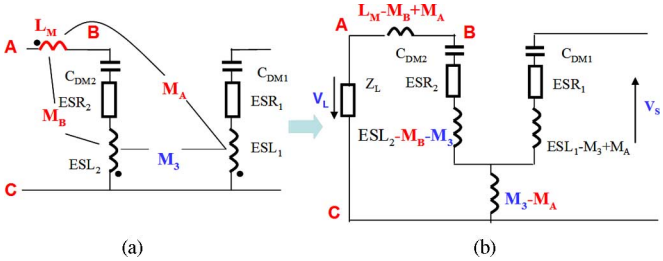

Fig. 11. Equivalent circuits for M_3 cancellation.

their values are much larger than the ESL of DM capacitors (for example, 89.3 nH versus 14 nH) [1], their effects are significant. It was proposed to rotate the inductor windings by 90° to minimize M_1 and M_2 [1]. After rotating, the magnetic flux of the DM inductors is symmetric to the center line of the DM capacitors, so the net coupling is very small. Fig. 9 shows this technique. In experiments, M_1 and M_2 are reduced by more than 90% from 89.3 to 7.5 nH [1].

It should be pointed out that since M_1 and M_2 are much larger than the ESL of DM capacitors, the DM filter's performance is not determined by ESL, as shown in Fig. 2.

D. Cancellation of the Mutual Inductance Between Two Capacitors

In Fig. 8, M_3 is the mutual inductance between two DM capacitors. Because the ratio of the currents in C_{DM1} and C_{DM2} is large (for example, 10^3 times) at HFs, a very small mutual inductance between these two DM capacitors can lead to performance degradation at HFs. M_6 is the mutual inductance between input and output trace loops. Its effects are as significant as those of M_3 for the same reason. At HFs, M_3 and M_6 provide a back door for noise, making it bypass the DM inductor. The left diagram in Fig. 10 illustrates the coupling between two DM capacitors. In the right diagram, a cancellation turn is proposed to be integrated with one DM capacitor C_{DM2} to cancel the effects of M_3 [8]. Fig. 11 shows the equivalent circuits for this cancellation.

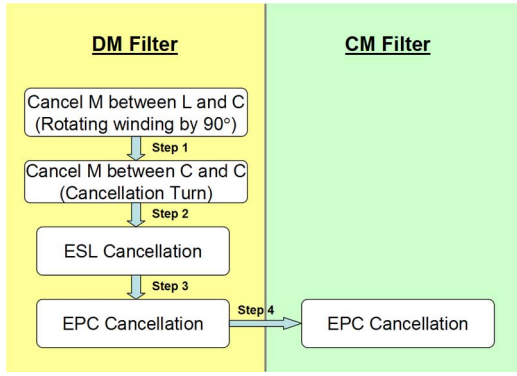

Fig. 12. Investigation of the possibilities of integrating parasitic cancellation techniques.

In Fig. 11, when the mutual inductance between the cancellation turn and the capacitor C_{DM1} is equal to the mutual capacitance M_3 between two capacitors, the effects of M_3 are canceled. The same technique can also be applied to two-stage EMI filters. Another benefit of a cancellation turn is that it also partially cancels the ESL of capacitor C_{DM2} [8].

An alternative method to reduce M_3 has been proposed by locating C_{DM1} and C_{DM2} in perpendicular planes [8]. M_3 can also be greatly reduced but it is not as good as a cancellation turn, because the filter footprint is increased. M_6 in Fig. 8 can be minimized by minimizing the input and output trace loop areas.

As stated earlier, for the investigated DM EMI filters, mutual couplings M_1–M_3 and M_6 have the most important influence on filter performance. Effects of ESL and EPC are not important, unless mutual couplings are minimized. For the investigated CM filter, on the contrary, the EPC of the CM inductors is the most important. Effects of mutual couplings may not be important because the CM magnetic flux is contained within cores.

III. Integration of Parasitic Cancellation Techniques

Both the self- and mutual parasitic cancellation techniques have been reviewed and their restrictions identified in Section II. In this section, the integration of these parasitic cancellation techniques for an EMI filter design with discrete components will be discussed. The investigation focuses on the restrictions of cancellation techniques when they are implemented in a filter system instead of a single component. The investigation also focuses on the interactions among different cancellation techniques. Since there are several cancellation techniques, for convenience, the investigation is carried out following the steps shown in Fig. 12.

A. Integration of Mutual Parasitic Cancellations for DM EMI Filters

It has been shown in Section II that there are two important mutual couplings in a one-stage DM EMI filter. One is the inductive coupling between inductors and capacitors. The other is the inductive coupling between the two capacitors. For a two-stage EMI filter, there is a third coupling, namely the inductive coupling between two inductors [1]. Since the inductive coupling between two inductors in a two-stage EMI filter is advantageous

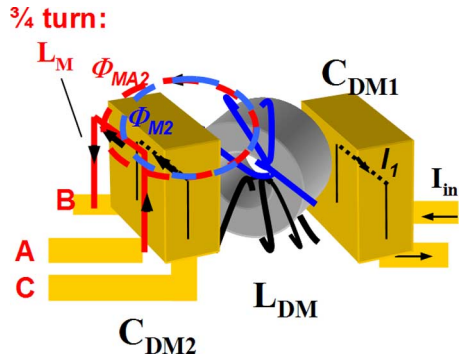

Fig. 13. Magnetic flux generated by the DM inductor links both the DM capacitor and the cancellation turn.

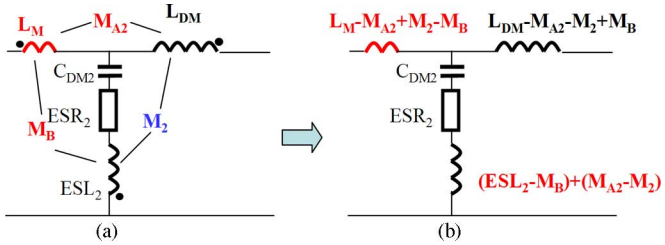

Fig. 14. Cancellation turn also helps to cancel the mutual inductance between the DM inductor and the DM capacitor.

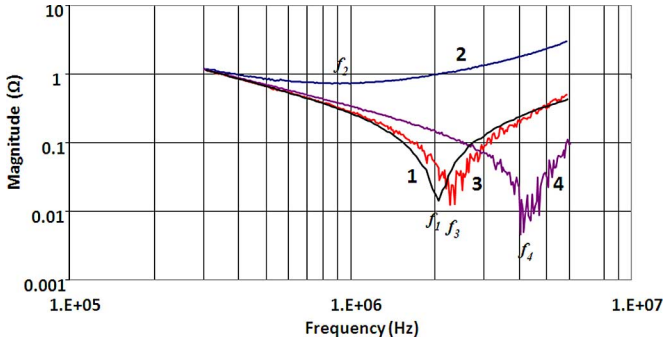

Fig. 15. Experimentally extracted impedances of a capacitor.

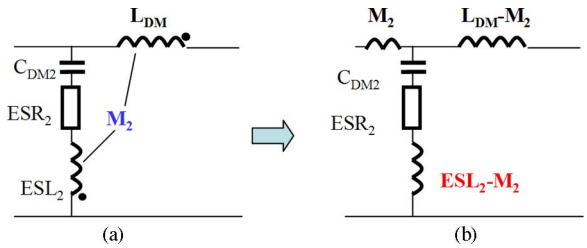

Fig. 16. Mutual couplings between an inductor and a capacitor. (a) Circuit. (b) Equivalent circuit.

to the filter's low-frequency performance improvement, it does not need to be canceled, so that only the cancellation of the first two mutual couplings will be discussed here.

As discussed in Section II, simply rotating an inductor's winding by 90° can greatly reduce the mutual coupling between the inductor and capacitors in the filter, since the leakage flux of the inductor is symmetric to the capacitors, reducing the net flux linking to the capacitors greatly. A cancellation turn integrated with a capacitor is introduced in Section II to cancel the mutual coupling M_3 between two capacitors. The basic principle for this method is that the induced voltage in the cancellation turn has a similar amplitude to that induced in the capacitor. At the same time, they have opposite directions so that their effects are canceled. It will be shown, with respect to Figs. 13 and 14, that the cancellation turn L_M integrated with the capacitor $C_{\rm DM2}$ can also help to cancel the mutual inductance between $L_{\rm DM}$ and $C_{\rm DM2}$.

In Fig. 13, the magnetic leakage flux Φ_{M2} links capacitor $C_{\rm DM2}$. Its effect is represented with the mutual inductance M_2 in Fig. 14(a). Since the cancellation turn L_M is very close to the capacitor, most of Φ_{M2} also links L_M. If this coupling is represented with mutual inductance $M_{\rm A2}$, the value of $M_{\rm A2}$ would be very close to M_2. The equivalent circuit for these couplings among $L_{\rm DM}$, $C_{\rm DM2}$, and cancellation turn L_M is shown in Fig. 14(b). With the aid of the network theory, three mutual couplings can be decoupled to obtain the network in Fig. 14(b).

In Fig. 14(a), the original ESL of capacitor $C_{\rm DM2}$ is $\rm ESL_2$. If there is no cancellation turn L_M, the inductance of the capacitor branch would be $\rm ESL_2$–M_2. After the inductor winding is rotated by 90°, M_2 is reduced greatly. If the cancellation turn L_M is integrated with capacitor $C_{\rm DM2}$, the cancellation turn L_M would have a mutual inductance $M_{\rm B}$ with capacitor $C_{\rm DM2}$. $M_{\rm B}$ can partially cancel $\rm ESL_2$ since the magnetic fluxes generated in the cancellation turn and the capacitor $C_{\rm DM2}$ cancel each other partially. The effect of $M_{\rm A2}$ on the capacitor branch is equivalent to increasing the inductance of the capacitor branch by $M_{\rm A2}$. Because $M_{\rm A2}$ is close to M_2 as discussed earlier, $M_{\rm A2}$ can cancel most of M_2. Based on this analysis, after L_M is integrated with capacitor $C_{\rm DM2}$, both the effects of $\rm ESL_2$ and M_2 are reduced greatly, as described in Fig. 14(b). The capacitor's HF filtering performance is thus further improved.

Experimental results are shown in Fig. 15 to verify the aforementioned analysis. The impedance of the capacitor $C_{\rm DM2}$ is first measured using an Agilent impedance analyzer. The measured impedance is the curve 1 in Fig. 15. There is a series resonance between $\rm ESL_2$ and $C_{\rm DM2}$ at frequency f_1 (2.07 MHz). The measured $C_{\rm DM2}$ is 461 nF, $\rm ESL_2$ is 12.8 nH, and $\rm ESR_2$ is 14.1 mΩ. In the second step, the scattering parameters of the network (an *LC* network with mutual inductance M between the inductor and the capacitor) in Fig. 16(a) are measured using a four-port, balanced RF network analyzer, Agilent E5070B. The impedance of the branch of capacitor $C_{\rm DM2}$ is extracted using measured scattering parameters [12]. Curve 2 in Fig. 15 is the extracted impedance curve that includes the effects of M_2. There is a minimal impedance at f_2. It is different from either the series or parallel resonant frequency [1]. Based on the theory developed in [1], the effects of the mutual inductance M_2 on the capacitor is equivalent to $-M_2$ in series with $\rm ESL_2$, as shown in Fig. 16(b). M_2 can be calculated since f_2 and $\rm ESL_2$ are known [12]. The calculated M_2 is -78.1 nH, and the sum of M_2 and ESL is -65.3 nH.

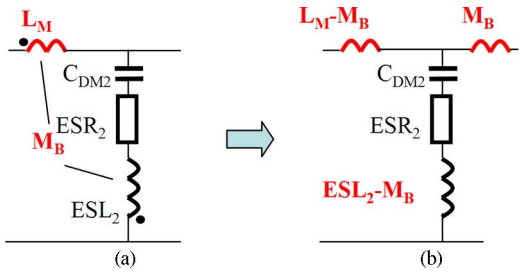

Fig. 17. ESL reduction with cancellation turn.

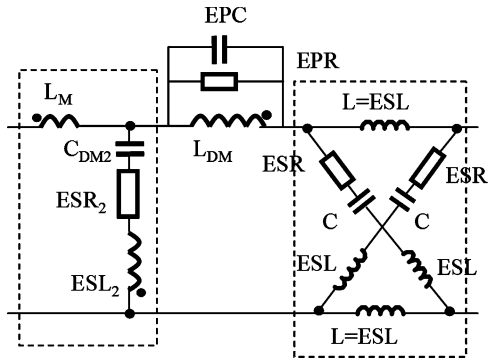

Fig. 18. EMI filter with cancellation turn and ESL cancellation.

In the third step, the inductor winding is rotated by 90° to reduce M_2. The scattering parameters are measured and the impedance of the capacitor branch is extracted. The curve 3 in Fig. 15 is the extracted impedance curve. It shows that the impedance is much lower than curve 2 at HF, which indicates a big performance improvement of the capacitor. There is a series resonance at frequency f_3 (2.3 MHz), which corresponds to a 10.4-nH inductance in the capacitor branch. In the last step, a cancellation turn L_M is integrated with the capacitor. The equivalent circuit for the mutual inductance $M_{\rm B}$, $L_{\rm M}$, and $\rm ESL_2$ is shown in Fig. 17(a). Fig. 17(b) shows $M_{\rm B}$'s effects on reduction of the ESL of the capacitor $C_{\rm DM2}$ [8]. The final equivalent circuit of the network with L_M added is represented by Fig. 14. The extracted impedance of the capacitor branch is shown as curve 4 in Fig. 15. The series resonant frequency is increased to f_4 at 4.4 MHz. The corresponding inductance in the capacitor branch is now 2.84 nH only. It is a 78% reduction of the inductance compared to the inductance in curve 1 (the impedance of the single capacitor) and a 95.7% reduction on inductance compared to the inductance in curve 2 (the impedance of a capacitor affected by the mutual coupling). This inductance reduction is due to the cancellation effects of the cancellation turn L_M on both $\rm ESL_2$ and M_2, as described by the diagram in Fig. 14(b). These experimental results verified that the cancellation can not only cancel $\rm ESL_2$ and M_3, but also M_2. As a conclusion, the two mutual coupling cancellation techniques of rotating the inductor winding by 90° and integrating a cancellation turn can be integrated simultaneously into an EMI filter design without any problems.

B. Integration of Self-Parasitic Cancellations

It has been shown in Section II that the self-parasitic cancellations can reduce the ESL of capacitors and the EPC of inductors when the effects of mutual couplings are insignificant. Although the self-parasitic cancellation could reduce self-parasitics, when the effects of mutual couplings are more significant than those of the reduced self-parasitics, the self-parasitic cancellation would be meaningless. Experiments are carried out in accordance with Fig. 18 to prove this.

In Fig. 18, the left box includes a capacitor with a cancellation turn L_M integrated. The right box includes two capacitors with the ESL cancellation technique (X–capacitor) applied. The top branch is the parasitic model of inductor $L_{\rm DM}$. As shown in Section II-A, the cancellation turn greatly improves the capacitor's HF performance, since it cancels both ESL and mutual couplings. It is therefore not necessary to add ESL cancellation (X–capacitor) to $C_{\rm DM2}$. Also, based on the theory of the cancellation turn, the cancellation turn should only be applied to one capacitor [8], so there is no need to integrate a cancellation turn with the capacitors on the right side.

There are two difficulties in integrating ESL cancellation with mutual coupling cancellations. First, the mutual inductance between $L_{\rm DM}$ and the X–capacitor is much larger than the canceled ESL even after the inductor winding is rotated by 90°. For example, although the mutual inductance between inductor $L_{\rm DM}$ and the capacitors can be reduced by up to 93% (from 80 to 7.5 nH) [1], its value is still much larger than the canceled ESL (around 1 nH) [3]. Second, the X–capacitor introduces one additional capacitor and two additional small inductors to the filter; as a result, more mutual couplings are introduced between capacitor $C_{\rm DM2}$ and the X–capacitor. The cancellation turn L_M is originally designed to cancel M_3 (see Fig. 8). More mutual couplings would make L_M more difficult to design. Following this reasoning, ESL cancellation by X–capacitor, used simultaneously with mutual coupling cancellation, does not readily lead to useful results. The problem is much more complicated than analyzed here and outside the scope of this paper.

The integration of the EPC cancellation for $L_{\rm DM}$ with cancellation of mutual coupling between the DM inductor and the DM capacitors also proves to be not a good choice. At first sight, it seems that the cancellation of the mutual couplings between the DM inductor and the DM capacitors can be integrated with the EPC cancellation of the DM inductor since one is related to the magnetic field and the other is related to the electric field. However, the practical situation is somewhat more complicated. The mutual inductance between the DM capacitors and the DM inductor actually affects both the DM capacitors and the DM inductor. Fig. 19 shows an example for analyzing this situation.

In Fig. 19(a), there is a mutual inductance M_2 between the DM inductor and the DM capacitor. If the current in the capacitor branch is I_1 and the current in the inductor is I_2, the effects of M_2 can be analyzed, as shown in Fig. 19(b). In this diagram, a current-controlled voltage source $j\omega M_2 I_1$ is in series with $L_{\rm DM}$. Since I_1 and I_2 have a difference of 40 dB/decade, at HFs, the amplitudes can be much different. As a result, at HF, the current-controlled voltage $j\omega M_2 I_1$ can be much larger than the voltage drop of I_2 on inductance $L_{\rm DM}$. If the voltage drop

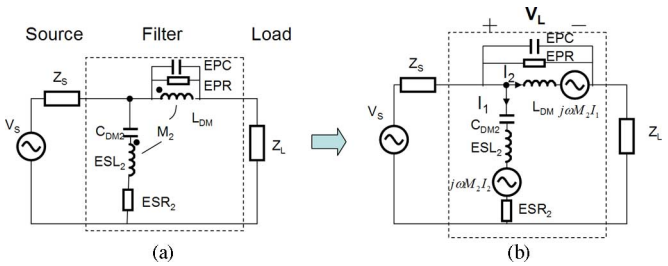

Fig. 19. Effects of the mutual inductance between an inductor and a capacitor on the inductor.

on the inductor is V_L, the effect of mutual inductance M_2 on the inductor can be described as

$$V_L = j\omega(LI_2 + M_2 I_1)$$

$$\text{IF } \frac{I_1}{I_2} \gg \frac{L}{M_2} \tag{1}$$

$$\Rightarrow V_L \approx j\omega M_2 I_1. \tag{2}$$

In Fig. 19(b), because I_1 and I_2 are not in phase, the characteristics of the inductor branch (EPC and EPR are not included) are very complicated at HFs. It can be either inductive or capacitive. It can also behave like a negative inductance or a negative capacitance. The amplitude of its impedance can even be proportional to f^3. A detailed analysis has been presented [11] but is not given here. Because of these effects on $L_{\rm DM}$, even with cancellation of EPC, $L_{\rm DM}$ still cannot behave like an ideal inductor. As a result, the filter's performance cannot be improved as expected. Although rotating the DM inductor winding by 90° can reduce M_2 by up to 93%, the coupling effects are still significant at HFs when I_1 and I_2 are significantly different. Because of this, integrating EPC cancellation with mutual coupling cancellations does not generally benefit the filter performance.

Three measurements are shown in Fig. 20 to verify the previous reasoning. Fig. 20(a) shows the configurations. The insertion gain of an *LC* filter is measured for each case and compared with the ideal case in Fig. 20. The measured EPC of the inductor is negative in these experiments. In case 1, the *LC* filter is composed of two parallel capacitors and an inductor. It is expected that the mutual coupling between the inductor and capacitors would significantly degrade the EMI filter's HF performance. The bump around 2 MHz is caused by the ESLs and the trace inductance between two capacitors. In case 2, the inductor winding is rotated by 90° to reduce the mutual inductance between the inductor and capacitors. The EMI filter's performance is improved over case 1 from 300 kHz to 20 MHz. In case 3, although the ESL cancellation technique is applied to two capacitors, the mutual inductance between the inductor and capacitors is much larger than the canceled ESL. The improvement of the filter performance is, therefore, limited, especially compared with the ideal case. The filter's performance is even worse than case 2 below 10 MHz. It should be pointed out that based on the analysis in [11], the mutual coupling between the inductor and capacitors modifies the behavior of the inductor. The inductor could behave like a negative inductance at HF. The impedance valley between 20 and 30 MHz in case 1 is actually caused by the resonance between this negative inductance and the EPC (negative)

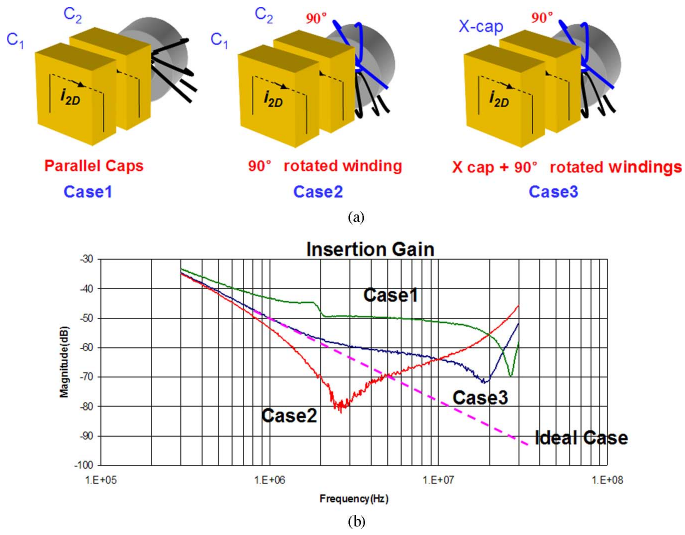

Fig. 20. Comparison of measured insertion gains. (a) Three configurations measured. (b) Comparison of measured insertion gains.

of the inductor. The impedance valley around 20 MHz in case 3 is also due to the same reason. On the other hand, the impedance valley around 2.5 MHz in case 2 is due to the series resonance in the capacitor branches with the effects of the coupling between the inductor and capacitors [11]. The experiments in Fig. 20 show that the effects of mutual couplings are dominant in either the capacitor branches or the inductor branch. The result of this is that the improvement of the self-parasitic cancellations on the filter performance is very limited. Furthermore, when the filter structure in Fig. 18 is considered, the mutual coupling between $C_{\rm DM2}$ and the X–capacitor would be another important restriction on the integration of self-parasiti cancellations.

For a CM filter with the circuit structure shown in Fig. 1, the EPC of the inductor is the most important parasitic to be canceled [2] since the effect of mutual coupling is not as significant as those in DM filters [2].

The mutual couplings in a DM filter do not affect the performance of its CM counterpart unless there are mode transformations between CM and DM noise due to unbalanced filter structures or parameters [9]. Basically, when asymmetry exists in the filter or any parts in the system, the DM and CM noise in the system can transfer to each other. The more asymmetric, the more mode transformation happens between DM and CM noise [9]. When the transformed noise is comparable to the noise without transformation, the effects of mode transformation cannot be ignored [9]. The mix-mode scattering parameters can be used to characterize this mode transformation. Because of this, if the system is perfectly symmetric (balanced), the cancellation for mutual couplings in DM filters does not make the EPC cancellation for the CM inductors in CM filters ineffective. They can certainly be integrated together.

Based on this reasoning, three types of parasitic cancellations can be integrated into one EMI filter. The first one is rotating the DM inductor winding by 90° to reduce M_1 and M_2 (see Fig. 8). The second one is integrating a cancellation turn with one DM capacitor to cancel M_3 (see Fig. 8). The third one is the EPC cancellation for CM inductors.

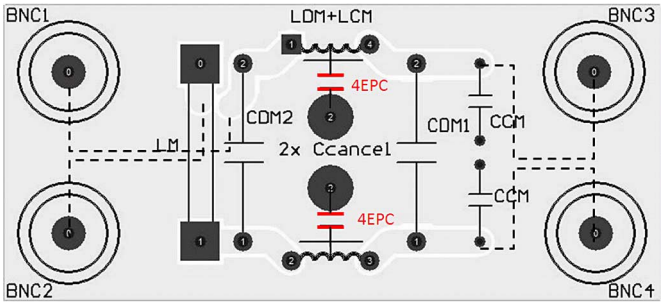

Fig. 21. PCB layout of the EMI filter with an integrated cancellation.

Although ESL cancellation and EPC cancellation for DM filters cannot be integrated with other mutual coupling cancellations, they can be applied to those applications when no significant mutual couplings are present. An example is that ESL cancellation can be applied to decoupling capacitors in a bus bar [13].

IV. Experimental Results on Integration of Parasitic Cancellation Techniques

An EMI filter with the structure given in Fig. 1 was built. The components used in the filter are the same components used in the measurements in Section III. For the DM inductor, $L_{\rm DM}$ is 19.5 μH, EPR is 38 kΩ, and EPC is -3.8 pF. For the CM inductor, $L_{\rm CM}$ is 3.1 mH, EPR is 14.5 kΩ, and EPC is 8.9 pF. For the DM capacitors, capacitance is 461 nF, ESL is 12.8 nH, and ESR is 14.1 mΩ. The two CM capacitors are 4.7 nF each. The PCB layout of the prototype is shown in Fig. 21, and measured insertion gains are compared in Fig. 22. All insertion gains and network parameters are measured using an Agilent four-port balanced network analyzer E5070B. The mutual parasitics are extracted using the methods reported in [12]. Three cases are investigated for the DM filter. For the first case, the DM filter's insertion gain is measured without any cancellation techniques applied. For the second case, the inductor winding is rotated by 90°, and it is found that M_2 is reduced from -78.1 to -2.4 nH. The DM filter performance is improved by several decibels after rotating the inductor winding by 90°. For the third case, the cancellation turn is integrated with one capacitor to cancel M_3. It is found that M_3 is reduced from 257 pH to 20 pH. There is 28 dB improvement at 30 MHz. The peak at 16 MHz on each curve is caused by the resonance between the DM capacitor $C_{\rm DM1}$ and the CM capacitors. The ESLs of DM and CM capacitors and the parasitic inductance of traces cause a series resonance in the loop of the DM and CM capacitors in Fig. 1. For the CM filter, the insertion gain of the filter with a conventional inductor winding structure is first measured without applying any CM parasitic cancellation techniques. The CM inductor is then replaced by a CM inductor with a bifilar winding structure [5], which maximizes the coupling coefficient of two winding halves so as to get the best cancellation [5]. Two grounded capacitors with a capacitance of 36 pF, which is almost four times the value of EPC, are connected to the center tap of the windings for EPC cancellation. The measured insertion gains are compared in Fig. 23. The CM filter's HF performance

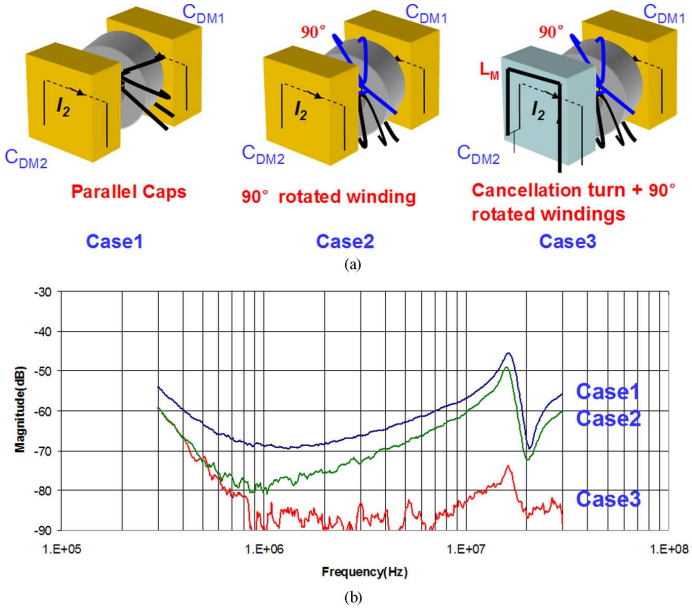

Fig. 22. Improvements of DM filter performance with parasitic coupling cancellations. (a) Three configurations measured. (b) Comparison of measured insertion gains.

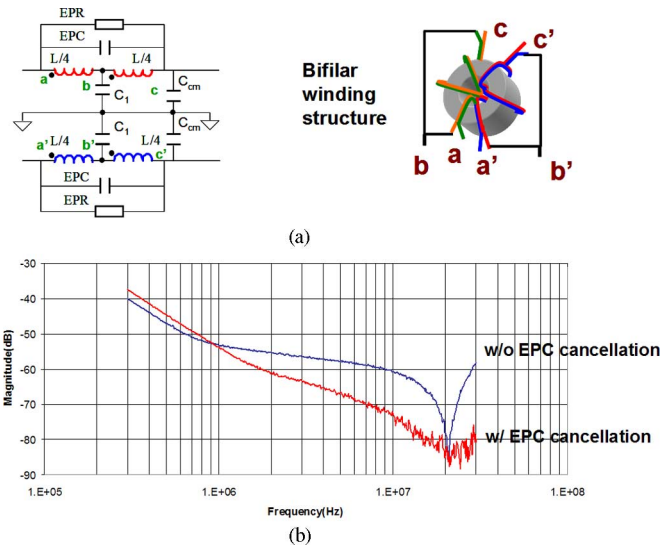

Fig. 23. Improvements of CM inductor performance with EPC cancellations. (a) CM circuit and inductor. (b) Comparison of measured insertion gains.

is improved by 20 dB at 30 MHz in Fig. 23. Measurements were also carried out to check the interactions between the DM parasitic and CM parasitic cancellations. As analyzed, it is found that no significant interactions were observed.

From Figs. 22 and 23, three parasitic cancellation techniques discussed in Section III can be integrated into one EMI filter without any conflicts and compromises. The HF performance of both DM and CM filters is improved greatly.

The integrated cancellation was also applied to a two-stage EMI filter. The experimental results are similar to those of the one-stage EMI filter shown earlier. It has been pointed out in Section III that ESL cancellation and EPC cancellation for DM capacitors and inductors can be applied to other

noise-suppression applications when mutual couplings are insignificant, such as to the input capacitor of a boost PFC converter.

V. Conclusion

In this paper, a range of parasitic cancellation techniques was selected and then reviewed. The possibilities of integrating these parasitic cancellation techniques into one EMI filter are analyzed. It was found that the EPC cancellation of the CM inductor can be integrated with the cancellation of the mutual inductance between the DM inductor and the DM capacitors, and with the cancellation of the mutual inductance between two DM capacitors. Experiments were carried out to prove this analysis. The experiments showed that by integrating three parasitic cancellation techniques into one EMI filter, the performance of both DM and CM filters is improved greatly. The ESL cancellation and EPC cancellation for DM capacitors and DM inductors can be used in those applications when mutual couplings are insignificant.

References

[1] S. Wang, F. C. Lee, D. Y. Chen, and W. G. Odendaal, "Effects of parasitic parameters on EMI filter performance," *IEEE Trans. Power Electron.*, vol. 19, no. 3, pp. 869–877, May 2004.

[2] S. Wang, R. Chen, J. D. van Wyk, F. C. Lee, and W. G. Odendaal, "Developing parasitic cancellation technologies to improve EMI filter performance for switching mode power supplies," *IEEE Trans. Electromagn. Compat.*, vol. 47, no. 4, pp. 921–929, Nov. 2005.

[3] S. Wang, F. C. Lee, and W. G. Odendaal, "Cancellation of capacitor parasitic parameters for noise reduction application," *IEEE Trans. Power Electron.*, vol. 21, no. 4, pp. 1125–1132, Jul. 2006.

[4] T. C. Neugebauer, J. W. Phinney, and D. J. Perreault, "Filters and components with inductance cancellation," *IEEE Trans. Ind. Appl.*, vol. 40, no. 2, pp. 483–490, Mar./Apr. 2004.

[5] S. Wang, F. C. Lee, and J. D. van Wyk, "Design of inductor winding capacitance cancellation for EMI suppression," *IEEE Trans. Power Electron.*, vol. 21, no. 6, pp. 1825–1832, Nov. 2006.

[6] T. C. Neugebauer and D. J. Perreault, "Parasitic capacitance cancellation in filter inductors," *IEEE Trans. Power Electron.*, vol. 21, no. 1, pp. 282–288, Jan. 2006.

[7] R. Chen, J. D. van Wyk, S. Wang, and W. G. Odendaal, "Improving the characteristics of integrated EMI filters by embedded conductive layers," *IEEE Trans. Power Electron.*, vol. 20, no. 3, pp. 611–619, May 2005.

[8] S. Wang, F. C. Lee, W. G. Odendaal, and J. D. van Wyk, "Improvement of EMI filter performance with parasitic coupling cancellation," *IEEE Trans. Power Electron.*, vol. 20, no. 5, pp. 1221–1228, Sep. 2005.

[9] S. Wang, "Characterization and cancellation of high-frequency parasitics for EMI filters and noise separators in power electronics applications," Ph.D. dissertation, Virginia Polytechnic Institute and State University, Blacksburg, VA, May 2005.

[10] R. Chen and J. D. van Wyk, "Planar inductor with structural winding capacitance cancellation for PFC boost converters," in *Proc. Appl. Power Electron. Conf.*, Mar. 2005, vol. 2, pp. 1301–1307.

[11] S. Wang and F. C. Lee, "Effects of mutual inductance between inductors and capacitors on LC filter performance," in *Proc. IEEE Power Electron. Spec. Conf.*, Jun. 2008, pp. 2615–2620.

[12] S. Wang, F. C. Lee, and W. G. Odendaal, "Characterization and parasitic extraction of EMI filters using scattering parameters," *IEEE Trans. Power Electron.*, vol. 20, no. 2, pp. 502–510, Mar. 2005.

[13] Q. Liu, S. Wang, F. Wang, C. Baisden, and D. Boroyevich, "EMI suppression in voltage source converters by utilizing DC-link decoupling capacitors," *IEEE Trans. Power Electron.*, vol. 22, no. 4, pp. 1417–1428, Jul. 2007.

[14] J. Neirynck, "Compensation of parasitic capacitances in broadband filters," *IEEE Trans. Circuit Theory*, vol. 14, no. 3, pp. 250–259, Sep. 1967.

[15] H. Chen, Z. Qian, Z. Zeng, and C. Wolf, "Modeling of parasitic inductive couplings in a Pi-shaped common mode EMI filter," *IEEE Trans. Electromagn. Compat.*, vol. 50, no. 1, pp. 71–79, Feb. 2008.

Shuo Wang (S'03–M'06–SM'07) received the B.S.E.E. degree from Southwest Jiaotong University, Chengdu, China, in 1994, the M.S.E.E. degree from Zhejiang University, Hangzhou, China, in 1997, and the Ph.D. degree from the Center for Power Electronics Systems (CPES), Virginia Polytechnic Institute and State University (Virginia Tech), Blacksburg, in 2005.

Since 2005, he has been a Research Assistant Professor at the Center for Power Electronics Systems, Virginia Tech. From 1997 to 1999, he was with ZTE Telecommunication Corporation, Shenzhen, China, where he was a Senior R&D Engineer and responsible for the development and support of the power supply for wireless products. In 2000, he was with UTstarcom Telecommunication Corporation, Hangzhou, where he was responsible for the development and support of the optical access networks. He holds one U.S. patent, and has three US patents pending.

Prof. Wang was the recipient of the 2005 Best Transaction Paper Award from the IEEE Transactions on Power Electronics and the William M. Portnoy Award for the best paper published in the IEEE Industry Applications Society (IAS) Annual Conference in 2004. He is an Associate Editor for the IEEE Transactions on Industry Applications.

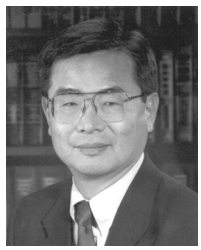

Fred C. Lee (S'72–M'74–SM'87–F'90) received the B.S. degree in electrical engineering from the National Cheng Kung University, Tainan, Taiwan, in 1968, and the M.S. and Ph.D. degrees in electrical engineering from Duke University, Durham, NC, in 1972 and 1974, respectively.

He is currently a University Distinguished Professor at Virginia Polytechnic Institute and State University, Blacksburg. He directs the Center for Power Electronics Systems (CPES), a National Science Foundation Engineering Research Center whose participants include five universities and over 80 corporations. He has authored or coauthored over 175 journal articles in refereed journals and more than 400 technical papers in conference proceedings. He holds 30 U.S. patents.

Prof. Lee was the recipient of the Society of Automotive Engineering's Ralph R. Teeter Education Award in 1985, the Virginia Tech's Alumni Award for Research Excellence in 1990, and the College of Engineering Dean's Award for Excellence in Research in 1997. In 1989, he received the William E. Newell Power Electronics Award. He was also the recipient of the Arthur E. Fury Award for Leadership and Innovation in Advancing Power Electronic Systems Technology in 1998 and the IEEE Millennium Medal.

Jacobus Daniel van Wyk (F'90) received the M.Sc. Eng. degree from the University of Pretoria, Pretoria, South Africa, in 1966, the Dr. Sc. Tech. (*cum laude*) degree from the Technical University, Eindhoven, Netherlands, in 1969, and the D.Sc. (Eng) (*honoris causa*) degree from the University of Natal, Durban, South Africa, in 1996.

He is currently with the Center for Power Electronics Systems, Virginia Polytechnic Institute and State University, Blacksburg, and also with the Department of Electrical and Electronic Engineering Science, University of Johannesburg, Johannesburg, South Africa. His current research interests include integrated electronic power processors, semiconductors, microelectronics, electric materials, electromechanical energy conversion, electric drives, power electronics, industrial electronics, control, alternative energy systems, electric vehicles, and many diverse applications in industry, mining, transportation, and electrical energy supply systems.

Dr. van Wyk is a Fellow of the South African Institute of Electrical Engineers. He was the recipient of 20 Prize Papers Awards, including 11 IEEE prize paper awards for some of his work, and the prestigious IEEE William E. Newell Power Electronics Award in 1995, and the IEEE Third Millennium Medal in 2000. He has received a range of other awards from IEEE Societies as well as from the South African Institute of Electrical Engineers. From 2002 to 2006, he was the Editor-in-Chief of the IEEE Transactions on Power Electronics.